DEVELOPMENT OF A NOVEL 3D HIGHER ORDER LAPLACIAN MODEL FOR ENHANCED PREDICTION OF WAVE IMPACT PRESSURE CALCULATION IN 3D MPS-BASED SIMULATIONS

Abbas Khayyer[1], Hitoshi Gotoh[2] and Hiroyuki Ikari[3]

[1]Dept. of Civil and Earth Resources Engineering, Kyoto University, khayyer@particle.kuciv.kyoto-u.ac.jp
[2]Dept of Civil and Earth Resources Engineering, Kyoto University, gotoh@particle.kuciv.kyoto-u.ac.jp
[3]Dept of Civil and Earth Resources Engineering, Kyoto University, ikari@particle.kuciv.kyoto-u.ac.jp

A 3D higher order Laplacian model is proposed for enhanced wave impact pressure calculation by the Moving Particle Semi-implicit (MPS) method. The Laplacian model is derived by meticulously taking the divergence of a SPH (Smoothed Particle Hydrodynamics) gradient model and is then utilized for discretization of Laplacian of pressure corresponding to the Poisson Pressure Equation (PPE). The enhancing and stabilizing effect of the 3D higher order Laplacian model is shown through simulations of designed exponentially excited sinusoidal pressure oscillations and a schematic dam break with an obstacle.

Key Words **:** *wave impact pressure, particle method, MPS, unphysical pressure fluctuations*

1. INTRODUCTION

As a Lagrangian gridless method, the MPS (Moving Particle Semi-implicit; Koshizuka and Oka, 1996) has been applied to a wide range of engineering applications, including coastal hydrodynamic flows. Despite its wide range of applicability, the MPS method has a few major drawbacks that may substantially affect its performance. Non-conservation of momentum (Khayyer and Gotoh, 2008), unphysical pressure fluctuations (Khayyer and Gotoh, 2009, 2010) and numerical instability (Khayyer and Gotoh, 2011) are among the major drawbacks associated with the MPS method.

Through the past couple of years, the authors have been working on enhancement of MPS method by revisiting the derivation of differential operator models and by proposing more accurate, consistent schemes, while trying to maintain the simplicity of the original method. Khayyer and Gotoh (2008) proposed a Corrected version of MPS method, abbreviated as CMPS, characterized by an anti-symmetric pressure gradient model. Later, a Higher order Source term, abbreviated as HS, was derived for enhancement of pressure calculation (Khayyer and Gotoh, 2009).

Another step towards enhancement and stabilization of pressure calculation by a projection-based particle method is to apply a more accurate Laplacian model for discretization of Laplacian of pressure in the Poisson Pressure Equation (PPE). Khayyer and Gotoh (2010) highlighted the importance of the mathematical consistency of the Laplacian model and discretized source term of the PPE and derived a 2D Higher order Laplacian model, abbreviated as HL, for the MPS method. In most cases, however, the mentioned enhanced particle methods have been applied to and verified by 2D calculations. On the other hand, most hydrodynamic flows are essentially three-dimensional. Hence, development of 3D accurate particle methods becomes indispensable.

The main aim of this study is to develop a 3D higher order Laplacian model for enhancement and stabilization of pressure field in 3D MPS-based simulations. The 3D Laplacian model is derived by meticulously taking the divergence of a commonly applied SPH (Smoothed Particle Hydrodynamics)

gradient model (Monaghan, 1992). It will be shown that the Laplacian model derived in a 3D framework differs to that corresponding to a 2D one and that the same approach can be applied for derivation of consistent Laplacian models in the SPH context. The enhancing effect of the 3D Laplacian model will be shown by simulating designed exponentially excited pressure oscillations (Khayyer and Gotoh, 2010, 2011) and a schematic dam break with an obstacle (Kleefsman et al., 2005).

2. DERIVATION OF A 3D LAPLACIAN

By considering the Laplacian at a target particle i as the divergence of the gradient calculated at that target particle and by applying the commonly applied SPH gradient model (Monaghan, 1992), the Laplacian at a target particle i would be formulated as (Khayyer and Gotoh, 2010):

$$\nabla\cdot\langle\nabla\phi\rangle_i=\frac{1}{n_0}\sum_{i\neq j}\left(\nabla\phi_{ij}\cdot\nabla w_{ij}+\phi_{ij}\nabla^2 w_{ij}\right) \tag{1}$$

In 3D Cartesian coordinates, the gradients of ϕ_{ij} and w_{ij} are expressed as:

$$\begin{aligned}\nabla\phi_{ij}&=\frac{\partial\phi_{ij}}{\partial r_{ij}}\frac{\partial r_{ij}}{\partial x_{ij}}\boldsymbol{i}+\frac{\partial\phi_{ij}}{\partial r_{ij}}\frac{\partial r_{ij}}{\partial y_{ij}}\boldsymbol{j}+\frac{\partial\phi_{ij}}{\partial r_{ij}}\frac{\partial r_{ij}}{\partial z_{ij}}\mathrm{k}\\ \nabla w_{ij}&=\frac{\partial w_{ij}}{\partial r_{ij}}\frac{\partial r_{ij}}{\partial x_{ij}}\boldsymbol{i}+\frac{\partial w_{ij}}{\partial r_{ij}}\frac{\partial r_{ij}}{\partial y_{ij}}\boldsymbol{j}+\frac{\partial w_{ij}}{\partial r_{ij}}\frac{\partial r_{ij}}{\partial z_{ij}}\boldsymbol{k}\end{aligned} \tag{2}$$

where $\phi_{ij}=\phi_j-\phi_i=-\phi_{ji}$ and $\nabla\phi_{ij}=\nabla\phi_j-\nabla\phi_i$. From Eq. (2):

$$\begin{aligned}\nabla\phi_{ij}\cdot\nabla w_{ij}&=\frac{\partial\phi_{ij}}{\partial r_{ij}}\frac{\partial r_{ij}}{\partial x_{ij}}\frac{\partial w_{ij}}{\partial r_{ij}}\frac{\partial r_{ij}}{\partial x_{ij}}+\frac{\partial\phi_{ij}}{\partial r_{ij}}\frac{\partial r_{ij}}{\partial y_{ij}}\frac{\partial w_{ij}}{\partial r_{ij}}\frac{\partial r_{ij}}{\partial y_{ij}}+\\ &\quad\frac{\partial\phi_{ij}}{\partial r_{ij}}\frac{\partial r_{ij}}{\partial z_{ij}}\frac{\partial w_{ij}}{\partial r_{ij}}\frac{\partial r_{ij}}{\partial z_{ij}}\\ &=\frac{\partial\phi_{ij}}{\partial r_{ij}}\frac{\partial w_{ij}}{\partial r_{ij}}\frac{x_{ij}^2}{r_{ij}^2}+\frac{\partial\phi_{ij}}{\partial r_{ij}}\frac{\partial w_{ij}}{\partial r_{ij}}\frac{y_{ij}^2}{r_{ij}^2}+\frac{\partial\phi_{ij}}{\partial r_{ij}}\frac{\partial w_{ij}}{\partial r_{ij}}\frac{z_{ij}^2}{r_{ij}^2}\\ &=\frac{\partial\phi_{ij}}{\partial r_{ij}}\frac{\partial w_{ij}}{\partial r_{ij}}\frac{x_{ij}^2+y_{ij}^2+z_{ij}^2}{r_{ij}^2}\\ &=\frac{\partial\phi_{ij}}{\partial r_{ij}}\frac{\partial w_{ij}}{\partial r_{ij}}=\frac{\phi_{ji}-\phi_{ij}}{r_{ij}}\frac{\partial w_{ij}}{\partial r_{ij}}=\frac{2\phi_{ji}}{r_{ij}}\frac{\partial w_{ij}}{\partial r_{ij}}\end{aligned} \tag{3}$$

On the other hand:

$$\begin{aligned}\nabla^2 w_{ij}=\nabla\cdot\nabla w_{ij}&=\frac{\partial}{\partial x_{ij}}\left(\frac{\partial w_{ij}}{\partial r_{ij}}\frac{\partial r_{ij}}{\partial x_{ij}}\right)+\frac{\partial}{\partial y_{ij}}\left(\frac{\partial w_{ij}}{\partial r_{ij}}\frac{\partial r_{ij}}{\partial y_{ij}}\right)\\ &\quad+\frac{\partial}{\partial z_{ij}}\left(\frac{\partial w_{ij}}{\partial r_{ij}}\frac{\partial r_{ij}}{\partial z_{ij}}\right)\\ &=\frac{\partial^2 w_{ij}}{\partial r_{ij}^2}\left(\frac{\partial r_{ij}}{\partial x_{ij}}\right)^2+\frac{\partial w_{ij}}{\partial r_{ij}}\frac{\partial^2 r_{ij}}{\partial x_{ij}^2}+\frac{\partial^2 w_{ij}}{\partial r_{ij}^2}\left(\frac{\partial r_{ij}}{\partial y_{ij}}\right)^2\\ &\quad+\frac{\partial w_{ij}}{\partial r_{ij}}\frac{\partial^2 r_{ij}}{\partial y_{ij}^2}+\frac{\partial^2 w_{ij}}{\partial r_{ij}^2}\left(\frac{\partial r_{ij}}{\partial z_{ij}}\right)^2+\frac{\partial w_{ij}}{\partial r_{ij}}\frac{\partial^2 r_{ij}}{\partial z_{ij}^2}\\ &=\frac{\partial^2 w_{ij}}{\partial r_{ij}^2}\frac{x_{ij}^2+y_{ij}^2+z_{ij}^2}{r_{ij}^2}+\frac{\partial w_{ij}}{\partial r_{ij}}\left(\frac{3}{r_{ij}}-\frac{x_{ij}^2+y_{ij}^2+z_{ij}^2}{r_{ij}^3}\right)\\ &=\frac{\partial^2 w_{ij}}{\partial r_{ij}^2}+\frac{2}{r_{ij}}\frac{\partial w_{ij}}{\partial r_{ij}}\end{aligned} \tag{4}$$

Comparing Eqs (3) and (4) with their corresponding equations in 2D framework (Eqs 11 and 12 in Khayyer and Gotoh, 2010), the only difference corresponds to the expression of Eq. (4), where the effect of space dimensionality is appeared in the summation of the terms including second partial derivatives of r_{ij} with respect to $\boldsymbol{r}_{ij}$. This would result in a different expression of Laplacian in 3D. From Eqs. (1), (3) and (4):

$$\begin{aligned}\nabla\cdot\langle\nabla\phi\rangle_i&=\frac{1}{n_0}\sum_{i\neq j}\left(\frac{2\phi_{ji}}{r_{ij}}\frac{\partial w_{ij}}{\partial r_{ij}}+\phi_{ij}\frac{\partial^2 w_{ij}}{\partial r_{ij}^2}+\frac{2\phi_{ij}}{r_{ij}}\frac{\partial w_{ij}}{\partial r_{ij}}\right)\\ &=\frac{1}{n_0}\sum_{i\neq j}\left(\phi_{ij}\frac{\partial^2 w_{ij}}{\partial r_{ij}^2}\right)\end{aligned} \tag{5}$$

It should be noted that the only simplification in derivation of the above higher order Laplacian model (from Eq. 1) corresponds to the considered first-order accurate finite difference approximation in Eq. (3), and all the other terms are exact expressions. By considering the standard MPS kernel, the higher order Laplacian in 3D would be simplified to:

$$\nabla\cdot\langle\nabla\phi\rangle_i=\frac{1}{n_0}\sum_{i\neq j}\left(\frac{2\phi_{ij}r_e}{r_{ij}^3}\right) \tag{6}$$

The 3D CMPS-HS with the above Higher order Laplacian will be referred to as 3D CMPS-HS-HL. **Table 1** summarizes the derived higher order Laplacian and its main comprising terms in 2D and 3D.

Table 1 Higher order Laplacian and its comprising terms

	2D	3D
$\nabla\phi_{ij}\cdot\nabla w_{ij}$	$\frac{2\phi_{ji}}{r_{ij}}\frac{\partial w_{ij}}{\partial r_{ij}}$	$\frac{2\phi_{ji}}{r_{ij}}\frac{\partial w_{ij}}{\partial r_{ij}}$
$\nabla^2 w_{ij}$	$\frac{\partial^2 w_{ij}}{\partial r_{ij}^2}+\frac{1}{r_{ij}}\frac{\partial w_{ij}}{\partial r_{ij}}$	$\frac{\partial^2 w_{ij}}{\partial r_{ij}^2}+\frac{2}{r_{ij}}\frac{\partial w_{ij}}{\partial r_{ij}}$
$\nabla\cdot\langle\nabla\phi\rangle_i$	$\frac{1}{n_0}\sum_{i\neq j}\left(\phi_{ij}\frac{\partial^2 w_{ij}}{\partial r_{ij}^2}-\frac{\phi_{ij}}{r_{ij}}\frac{\partial w_{ij}}{\partial r_{ij}}\right)$	$\frac{1}{n_0}\sum_{i\neq j}\left(\phi_{ij}\frac{\partial^2 w_{ij}}{\partial r_{ij}^2}\right)$

3. VERIFICATIONS

The enhancing effect of the 3D higher order Laplacian model is demonstrated by performing two numerical tests, namely, designed exponentially excited sinusoidal pressure oscillations (Khayyer and Gotoh, 2010, 2011) and a schematic dam break with an obstacle (Kleefsman, 2005). To make the comparisons more comprehensible, the fluid is considered to be inviscid so that the stabilizing effect of the viscous forces will be entirely omitted.

(1) Designed Exponentially Excited Sinusoidal Pressure Oscillations

Hydrostatic pressure calculations with designed exponentially excited sinusoidal pressure oscillations have been carried out to verify the enhanced performance of 3D CMPS-HS-HL method. The calculation conditions are as follows: d_0 = particle diameter = 1.0E-2 m and Δt = 1.0E-3 s. The water tank is a cube of 0.18 m with the water depth being 0.16 m. The modified gravitational acceleration is defined as:

$$\boldsymbol{g}_d = \boldsymbol{g} + \frac{\boldsymbol{g}}{2}\mathrm{Sin}\left(\frac{2\pi t}{T}\right)\exp(0.03\frac{\pi t}{T}) \qquad (7)$$

where $\boldsymbol{g}_d$ represents designed external accelerations applied to fluid particles; $\boldsymbol{g}$ is the earth's gravitational acceleration (= −9.81 m/s^2); t stands for the simulation time and T denotes the period of sinusoidal term variations (= 0.02 s).

Fig. 1 shows the snapshots of water particles together with the pressure field at t = 0.245 s. At this instant, the spatial distribution of pressure by the 3D CMPS-HS-HL method appears to be almost consistent with a hydrostatic pressure distribution. In contrast, the 3D CMPS-HS method has depicted an unphysical spurious pressure distribution characterized by several zero-pressure inner fluid particles.

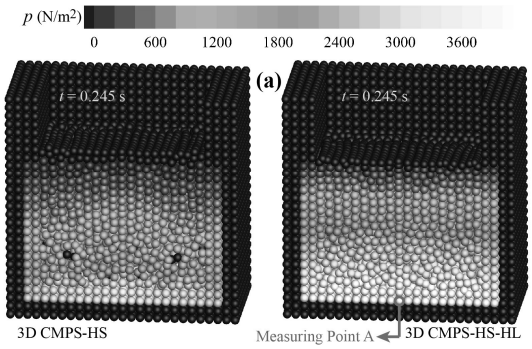

Fig. 1 Snapshots of water particles and pressure field

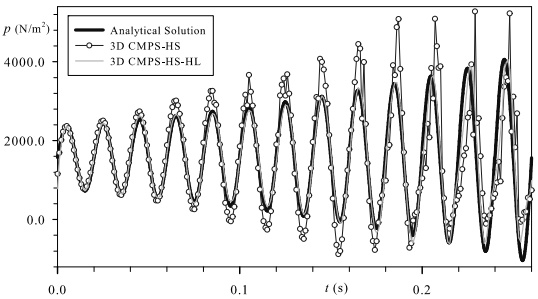

Fig. 2 Time histories of pressure at measuring point A (Fig. 1)

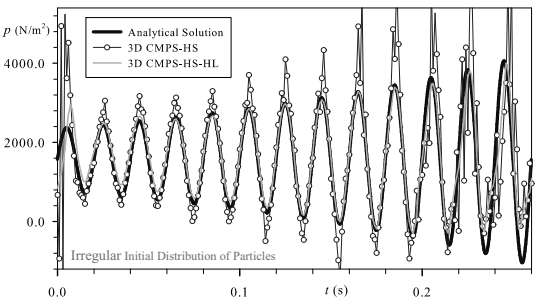

Fig. 3 Time histories of pressure at measuring point A (Fig. 1) for irregular initial distribution of particles

Fig. 2 depicts the time histories of pressure at a fixed point (measuring point A in **Fig. 1**) by 3D CMPS-HS and 3D CMPS-HS-HL methods. In spite of relatively accurate approximations at the beginning of the calculation, the pressure calculation by the 3D CMPS-HS has become destabilized after a few periods of designed oscillations. The 3D CMPS-HS-HL method, on the other hand, has provided a notably more accurate and stable pressure calculation.

Fig. 3 illustrates the time variations of calculated pressure at point A when the initial distribution of particles is randomly altered and half of fluid particles are displaced by $\pm 0.05d_0$ in both x and y directions. As a result of an irregular distribution of

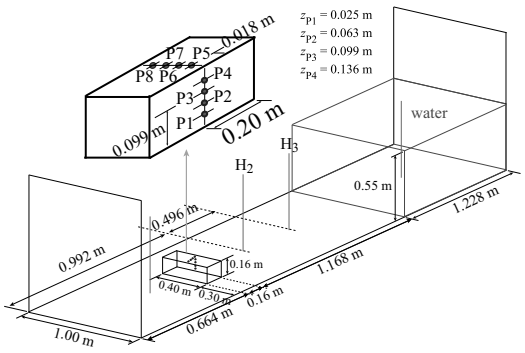

Fig. 4 Schematic sketch of domain - dam break with obstacle

particles (an initial compression or expansion and violation of fluid incompressibility), the pressure results by both methods appear to deviate from the analytical solution at the beginning of the calculation. This deviation tends to be smooth and relatively stable in case of the 3D CMPS-HS-HL method. In contrast, the pressure trace by the 3D CMPS-HS method is initiated by frequent large-amplitude unphysical oscillations. After one period of oscillation, the results by both methods seem to become closer to the analytical solution. However, the 3D CMPS-HS results still appear to be inaccurate and inconsistent, particularly, in the vicinity of the peak and trough points. In contrast, the 3D CMPS-HS-HL tends to provide a relatively stable and accurate pressure calculation and the growth of instabilities tends to be less pronounced when the HL scheme is incorporated.

(2) A Schematic Dam Break with an Obstacle

Schematic dam break flows have been commonly used for the verification of numerical methods. An experiment on a schematic dam break flow and its impact against an obstacle, carried out at the MAritime Research Institute Netherlands (MARIN), has been considered as a benchmark test for the validation of both 3D particle methods and 3D grid-based methods. A schematic sketch of the calculation domain including the positions of the wave height probes and pressure sensors installed in the experiment is depicted in **Fig. 4**. Detailed descriptions of the experiment have been provided by Kleefsman et al. (2005). For all the calculations performed in this section, d_0 is set to be 2.0E-2 m, resulting in a total number of 215940 particles.

Fig. 5 presents a qualitative comparison in between 3D CMPS-HS and 3D CMPS-HS-HL by illustrating snapshots of water particles together with the pressure field at t = 0.49 s. From this figure, it is evident that application of the new Laplacian

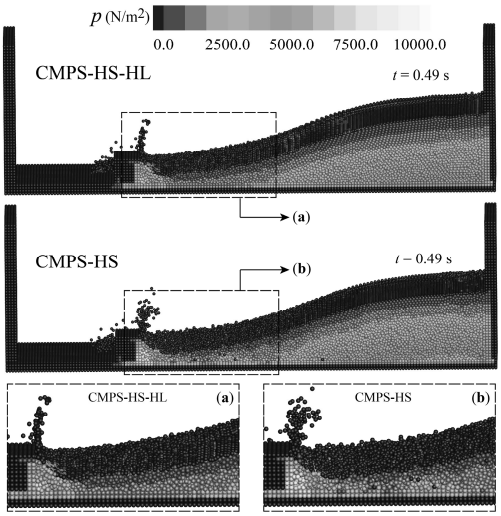

Fig. 5 Qualitative comparison in between 3D CMPS-HS and 3D CMPS-HS-HL at t = 0.49 s - dam break with obstacle

model has significantly reduced the existing numerical noise seen in the 3D CMPS-HS snapshot. Further, the 3D CMPS-HS-HL has also resulted in a more integrated water jet.

Fig. 6(a-d) presents a qualitative comparison in between simulation and experiment at t = 0.56 s. Comparing **Fig. 6(a-b)** with (**c**), the 3D CMPS-HS-HL has provided a more integrated jet. Moreover, from **Fig. 6(a)** and (**c**), the height of the jet and other macroscopic features of flow, e.g. backward curl of the jet towards the incoming flow, appear to be in acceptable qualitative agreement with the experiment. From **Fig. 6(d)**, the high order VOF method of Kleefsman (2005) has resulted in a straight fully integrated jet and the backward curl has not been reproduced well.

Fig. 7(a-b) depicts time histories of experimental and calculated pressures at measuring points P1 and P5 (**Fig. 4**). The figure shows the step-by-step improvements in pressure calculation by incorporating the higher order source term and the higher order Laplacian model. Compared with the 3D CMPS-HS, the 3D CMPS-HS-HL method has resulted in a less-fluctuating, more-accurate pressure trace in a better agreement with the experiment. In particular, a more consistent calculation of the peak pressure rise and declination (**Fig. 7(a)**) is illustrated by the 3D CMPS-HS-HL method. The high-order VOF method of Kleefsman et al. (2005) has resulted in quite smooth variations of pressure. Nevertheless, the pressure traces by this high-order grid-based method are characterized by some instabilities particularly at the impact instants.

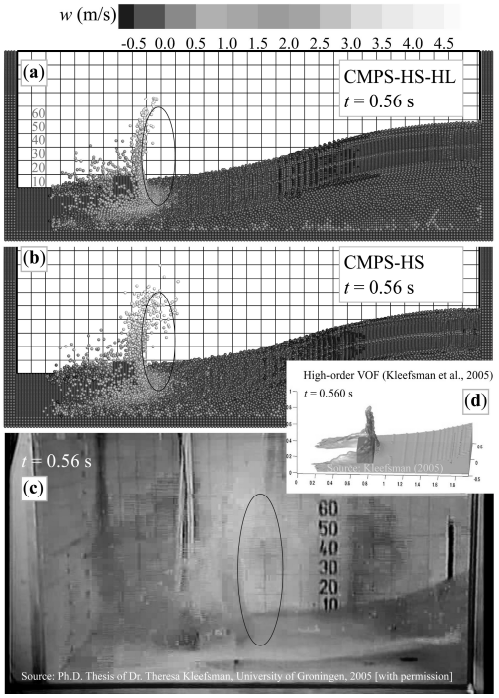

Fig. 6 Qualitative comparison in between 3D CMPS-HS, 3D CMPS-HS-HL and experiment and VOF (Kleefsman et al., 2005) at $t = 0.56$ s - dam break with obstacle

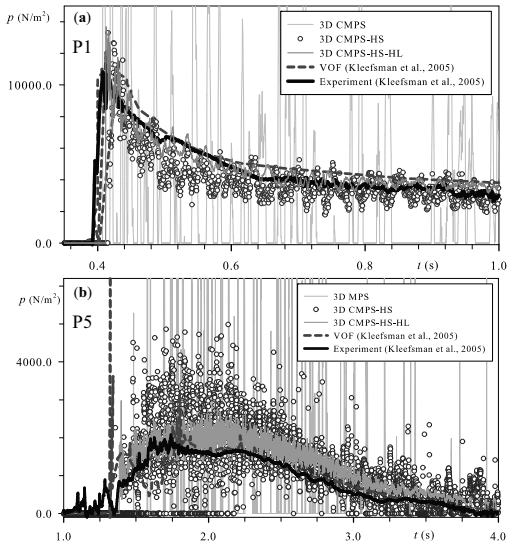

Fig. 7 Time histories of calculated and experimental (Kleefsman, 2005) pressure at measuring points P1 and P5 (Fig. 4)

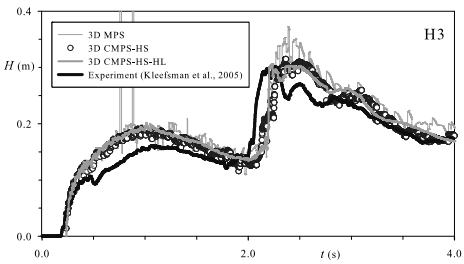

Fig. 8 Time histories of water surface height at probe H3 (Fig. 4) - dam break with obstacle

Fig. 8 depicts the time variations of water surface height at probe H3 and shows the step-by-step enhancing effects of the higher order source term and the higher order Laplacian in providing smoother and more accurate time variations of water surface height.

4. CONCLUDING REMARKS

A 3D higher order Laplacian model is proposed for further enhancement of wave impact pressure calculation in 3D particle-based simulations. The new Laplacian is derived by meticulously taking the divergence of a particle-based gradient model. The enhancing effect of the 3D Laplacian model is shown by simulating designed sinusoidal pressure oscillations together with a schematic dam break with an obstacle.

REFERENCES

Koshizuka, S. and Y. Oka (1996): Moving particle semi-implicit method for fragmentation of incompressible fluid, *Nuclear Science and Engineering*, 123, 421-434.

Khayyer, A. and H. Gotoh (2008): Development of CMPS method for accurate water-surface tracking in breaking waves, *Coastal Eng. J.*, 50(2), 179-207.

Khayyer, A. and H. Gotoh (2009): Modified Moving Particle Semi-implicit methods for the prediction of 2D wave impact pressure, *Coastal Eng.*, 56(4), 419-440.

Khayyer, A. and H. Gotoh (2010): A Higher Order Laplacian Model for Enhancement and Stabilization of Pressure Calculation by the MPS Method, *Applied Ocean Research*, 32(1), 124-131.

Khayyer, A. and H. Gotoh (2011): Enhancement of stability and accuracy of the Moving Particle Semi-implicit method, *Journal of Computational Physics*, 230(8), 3093-3118.

Monaghan, J.J. (1992): Smoothed particle hydrodynamics, *Ann. Rev. Astron. Astrophys*, 30(1), 543-574.

Kleefsman, K.M.T., Fekken, G., Veldman, A.E.P., Iwanowski B. and B. Buchner (2005): A Volume-of-Fluid based simulation method for wave impact problems, *Journal of Computational Physics*, 206, 363-393.

Kleefsman, K.M.T. (2005): Water Impact Loading on Offshore Structures, A Numerical Study, Ph.D. thesis, University of Groningen, The Netherlands, November.

(Received June 15, 2012)